to run the simulations. The cooperative control law will be evaluated under different network topologies, for the microgrid described in Section 6, with simulation results shown in Section 7. Finally, Section 8 will address the conclusions of the simulation runs.

## 2. Control hierarchy on Microgrids

A microgrid should be able to operate in two modes: in island mode, disconnected from the utility grid, and in grid-connected mode, connected to a larger power system through the PCC [5]. In island mode, the active and reactive power generated by the distributed generation of the microgrid, should equal the demand of local loads. Voltage and frequency of the microgrid are no longer supported by the host grid and, therefore the Distributed Energy Resources (DER) must keep them under control. In grid-connected mode, the frequency of the microgrid and the voltage at the PCC are maintained by the stiffness of the utility grid. In this mode of operation, the power deficit within the microgrid can be supplied by the utility grid, and the excess power generated in the microgrid can be traded with the utility grid.

Islanded operation of the microgrid could be planned, or unplanned if a fault triggers the disconnection of the microgrid from the utility grid. The transitions between modes of operation should be handled in a safe and smooth way.

Microgrid control has been proposed in three levels by several researchers [6]: (a) Primary Control, (b) Secondary Control and (c) Tertiary Control. The actual current or voltage control of the VSCs is, typically, excluded from this list, because it has nothing to do with the microgrid operation and it is often called zero control level.

## 3. Primary Control: Droop Control

Primary control shapes the initial response of each generator when a disturbance takes place.

*A. V/f source converters*

In each VSC (i) of a microgrid working as a voltage source, the following primary frequency and voltage control laws are usually proposed:

$$f_i = f_o - K_{pi}(P_i - P_{io}) \quad (1)$$
$$V_i = V_o - K_{qi}(Q_i - Q_{io}) \quad (2)$$
$$\text{for } i = 1,2,\cdots,n$$

where *f* stands for frequency, *P* stands for active power and *Q* stands for reactive power. Subscript (o) points at an initial equilibrium point in which there was perfect equilibrium between generated and consumed P and Q, and *Kp* and *Kq* are the droop gains for frequency and voltage control, respectively.

The equations above imitate, artificially, the behaviour of a traditional synchronous generator. When a generator's P load increases [decreases], the output frequency (generator's speed) is reduced [is increased]. Similarly, when the generator's Q load increases [decreases] the generator terminal voltage decreases [rises] due to the voltage drop in its internal impedance. The so-called "droop" control laws in (1) and (2) rely on the fact that, typical electrical grids and loads show a positive sensitivity in P and Q consumed with respect to frequency and voltage, respectively ($\Delta P/\Delta f > 0;\ \Delta Q/\Delta V > 0$) and, therefore, (1) and (2) close a control loop with negative feedback.

*B. P/Q source converters*

In this case, "droop" controllers take the form of:

$$P_j = P_o - K_{fj}(f_j - f_{jo}) \quad (3)$$
$$Q_j = Q_o - K_{vj}(V_j - V_{jo}) \quad (4)$$
$$\text{for } j = 1,2,\cdots,m$$

This time, the droop used in each VSC (j) is also based on the behaviour of conventional electrical grids. If, for example, a decrease in frequency is detected, each VSC is asked to increase its P production. Similarly, if a voltage drop is detected, each VSC is asked to increase its Q production. Each VSC will control the magnitude and orientation with respect to the bus voltage of its output current so that the requested values of $P_j$ and $Q_j$ are satisfied. The orientation of the converter output current needs the application of a phase-locked-loop algorithm in order to detect where the bus voltage vector is.

When V/f source converters are parallel connected, droop gains (*Kpi* and *Kqi*) are selected by balancing inverter apparent power (S) ratings [7]; in such a way that the inverter with the highest rating will be the one providing more power to go back to a balanced situation:

$$K_{pi}P_i = K_{p(i+1)}P_{(i+1)} \quad (5)$$
$$K_{qi}Q_i = K_{q(i+1)}Q_{(i+1)} \quad (6)$$

When P/Q source converters are parallel connected with V/f source converters, "droop" gains (*Kfj* and *Kvj*) are also selected in a way that the inverter with the highest rating will be the one providing more power to go back to a balanced situation:

$$K_{pi}P_i = \frac{P_j}{K_{fj}} \quad (7)$$
$$K_{qi}Q_i = \frac{Q_j}{K_{vj}} \quad (8)$$

Equations (1)-(4) are proportional control laws which will drive the system (if stable) to an operating point with a frequency and a bus voltage profile different from the required ones. This error must be corrected by the secondary control.

## 4. Secondary Control: Distributed Cooperative Control

Secondary control techniques for frequency and voltage restoration in island microgrids, is a topic that has not been addressed as often as droop control. There are mainly two approaches for secondary control, one based on centralized techniques equivalent to a master/slave control scheme, which requires one-to-all communication with a low bandwidth channel; and a second approach based on decentralized techniques equivalent to a multi-master control scheme (or cooperative control), which requires communication among agents with a high bandwidth channel to hold all telegrams between the converters. Both techniques must provide reliable operation of the microgrid, and robustness against communication failures and unknown communications delays [8].

Centralized control techniques use conventional approaches like proportional integral PI controllers, which provide a secondary control level with slow response (1-2 minutes). As already reported by [9], reactive power sharing of Q-V droop control is hard to achieve, since unlike frequency, the voltage is not the same along the several buses within the microgrid. A drawback of the centralized approach, is that a communication failure on the centralized controller will stop the secondary control action,

losing frequency and voltage restoration, in spite of maintaining primary control with local information.

Decentralized control techniques are becoming popular nowadays, and not only for microgrids. In decentralized control systems, the main responsibility is given to local controllers or agents. Agents are basically sophisticated computer programs that act autonomously on behalf of their users, across open and distributed environments, to solve a growing number of complex problems. A multi-agent system is a network of software agents that interact with each other with the ability to coordinate, negotiate and cooperate with other agents to achieve a common goal.

Cooperative control studies the dynamics of multi-agent dynamical systems linked to each other by a communication graph. The graph represents the allowed information flow between the agents, where each agent is confined to depend only on its own information and the information provided by its neighbours in the graph [10].

It was Reynolds [11] the first to propose a computer animation model to simulate collective behaviour of multiple agents, and after him several researches have provided some new in-sites of systematic framework of consensus problems. While most literature concentrates on studying consensus under a fixed communication topology, in some applications the communication topology might change due to communication range limitations, mainly when agents are moving in space, like in the case of flight formation or robot synchronization.

The control laws for each VSC in a microgrid have been extended with a cooperative control law where the microgrid takes the form of a multi-agent dynamic system, where agents are interconnected by a "fixed" topology communication network defined by its graph, and each agent or node is mathematically modelled by a dynamical linear time-invariant system, with communication delays being neglected [12].

### *A. Algebraic Graph Theory*

The communication network is modelled by a graph and establishes the links and interconnections between the agents. The graph consists of nodes representing the agents, and directed edges corresponding to the allowed flow of information between the agents. Some basic graph theory concepts [13] are essential in the study of multi-agent dynamical systems.

A *weighted order n graph* is defined as a pair $\boldsymbol{G} = (\boldsymbol{V}, \boldsymbol{E})$, with a finite nonempty set of *n* nodes $V = \{v_1, \cdots, v_n\}$, a set of edges or arcs $\boldsymbol{E} \subseteq \boldsymbol{V} \times \boldsymbol{V}$, and a weighted adjacency matrix $\boldsymbol{A} = (\boldsymbol{a_{ij}})_{\boldsymbol{n}\times\boldsymbol{n}}$.

The *weighted in-degree* of a node $\boldsymbol{v_i}$ is the sum of the weights of edges having $\boldsymbol{v_i}$ as a head, so it will be equal to the i-th row sum of $\boldsymbol{A}$:

$$d_{in} = \sum_{j=1}^{n} a_{ij} \tag{9}$$

And the *weighted out-degree* of a node $\boldsymbol{v_i}$ is the sum of weights of edges having $\boldsymbol{v_i}$ as a tail, so it will be equal to the j-th column sum of $\boldsymbol{A}$:

$$d_{out} = \sum_{i=1}^{n} a_{ij} \tag{10}$$

The in-degree and out-degree are local properties of the graph. A *(directed) tree* is a connected digraph where every node except one, called the root, has in-degree equal to one. A *spanning tree* of a digraph is a directed tree formed by graph edges that connects all the nodes of the graph. A graph is said to have a spanning tree, if a subset of the edges forms a directed tree meaning that there is a node (called *root node*) with a direct path from that node to every other node in the graph with no cycles (a cycle is a simple path that starts and ends at the same node). The root set or leader set of a graph is defined as the set of nodes that are the roots of all spanning trees. A graph may have multiple trees; however, if it contains at least one spanning tree, the graph is declared as strongly connected.

The adjacency matrix $\boldsymbol{A}$ of an undirected graph is symmetric, $\boldsymbol{A} = \boldsymbol{A^T}$. A graph is said to be *weight balanced* if the weighted in degree equals the out-degree for all i. If all the nonzero edge weights are equal to 1, this is the same as the definition of balanced graph. An undirected graph is weight balanced, since if $\boldsymbol{A} = \boldsymbol{A^T}$, then the i-th row sum equals the i-th column sum.

The *Graph Laplacian matrix* is defined as follows:

$$L = D - A \tag{11}$$

where $\boldsymbol{D} = \boldsymbol{diag}\{\boldsymbol{d_{in}}\}$ is the in-degree matrix, and $\boldsymbol{A}$ the adjacency matrix. Note that L has all row sums equal to zero.

Many properties of a graph may be studied in terms of its graph Laplacian matrix, providing a key role in the analysis of dynamical multi-agent systems on graphs. The eigenvalues of the Laplacian matrix explain properties of the underlying graph topology.

When multiple agents agree on the value of a variable of interest, they are said to have reached consensus. Consensus algorithms are designed to be distributed, assuming only neighbour-to-neighbour interaction between agents, so agents will update the value of their information based on the information of their neighbours. Hence, the goal will be to design an updated law, so that the information of all agents in the network converge to a common value.

Consensus algorithms have been studied extensively in the context of cooperative control of multi-agents. The most general continuous time consensus algorithm was formulated by [14], and it is given by the first order single integrator dynamics:

$$\frac{d}{dt}(x_i) = \sum_{j=1}^{n} a_{ij}[x_j - x_i] \tag{12}$$

where $a_{ij}$ is the (i j) entry of the adjacency matrix $\boldsymbol{A} \in \boldsymbol{R^{n\times n}}$ of a digraph $\boldsymbol{G}$, and $\boldsymbol{x_i}$ is the information of the i-th agent. Setting $a_{ij} = 0$ denotes the fact that agent i cannot receive information from agent j. A consequence of equation (8) is that the information of agent i is driven toward the information of its neighbours.

Equation (12) can be written in matrix form, considering the global dynamics of the state vector $x = [x_1 \cdots x_n]^T \in R^n$ as:

$$\frac{d}{dt}(x) = -[D - A]x \tag{13}$$

### *B. Cooperative Control Algorithm*

The secondary control for frequency restoration based on a distributed cooperative tracker algorithm, has to be applied exclusively among the *V/f* source converters as follows:

$$f_i = f_o - K_{pi}(P_i - P_{io} + \partial P_i^{ter}) + \partial f_i^{sec} + \partial f_i^{sync} \quad (14)$$

$$\frac{d}{dt}(\partial f_i^{sec}) = -k_f[\eta_1 + \eta_2 + \eta_3] \quad (15)$$

$$\eta_1 = \sum_{l=1}^{n} a_{il}(f_i - f_l) \quad (16)$$

$$\eta_2 = g_i(f_i - f_{ref}) \quad (17)$$

$$\eta_3 = \sum_{l=1}^{n} a_{il}(K_{pi}P_i - K_{pl}P_l) \quad (18)$$

$$\text{for } i = 1,2,\cdots,n$$

where, $\partial f_i^{sec}$ is the contribution of the secondary control (frequency tracking error), $\partial P_i^{ter}$ is the contribution of the tertiary control (to be explained later) and $\partial f_i^{sync}$ is the contribution of the algorithm for the synchronization with the utility grid. Besides, $k_f$ is the secondary frequency control gain, $a_{ij}$ are the elements of the adjacency matrix defined by the graph network topology, $g_i$ is the pinning gain ($g_i \neq 0$, only for the leader agent who has the set-point for the system frequency), and $\partial f_i^{sec}$ is the frequency tracker error.

Voltage secondary control, to match a voltage profile defined at the converter connection buses, based on distributed cooperative tracker algorithm, has to be implemented among V/f and P/Q source converters as follows:

$$V_i = V_o - K_{qi}(Q_i - Q_{io}) + \partial V_i^{sec} \quad V/f \text{ source} \quad (19)$$

$$Q_j = Q_o - K_{vj}(V_j - V_{jo} - \partial V_j^{sec}) \quad P/Q \text{ source} \quad (20)$$

$$\frac{d}{dt}(\partial V_t^{sec}) = -k_v[\mu_1 + \mu_2 + \mu_3] \quad (21)$$

$$\mu_1 = \sum_{l=1}^{n+m} a_{tl}(V_t - V_l) \quad (22)$$

$$\mu_2 = g_t(V_t - V_{ref}) \quad (23)$$

$$\mu_3 = \sum_{l=1}^{n+m} a_{tl}(K_{qt}Q_t - K_{ql}Q_l) \quad (24)$$

$$\text{for } i = 1,2,\cdots,n$$
$$\text{for } j = 1,2,\cdots,m$$
$$\text{for } t = 1,2,\cdots,n+m$$

where $\partial V_i^{sec}$ is the contribution of the secondary voltage control (voltage tracking error), $k_v$ is the secondary voltage control gain and $a_{ij}$ and $g_i$ are as defined before. However, in this case, several VSC can be made leaders to guarantee the required voltage at several buses. As already noticed by [15], a trade-off between the conflicting goals of voltage regulation and reactive power sharing needs to be reached.

### C. *Voltage synchronization at the PCC*

Before connecting the microgrid to the utility grid, the voltage (magnitude and phase) at the microgrid side of the PCC must be synchronized with the utility grid side. The term $\partial f_i^{sync}$ in (14) can be added to all *V/f* with an integral term making.

$$\frac{d}{dt}(\partial f_i^{sync}) = -k_{pcc}(\theta_{pcc} - \theta_{ref}) \quad (25)$$

$$\text{for } i = 1,2,\cdots,n$$

## 5. Tertiary control

The tertiary control should ensure a given active power profile for all converters (V/f and P/Q sources), which will be the solution of an optimum power flow, for the point of operation of the microgrid. This can be achieved by adding the term $\partial P_i^{ter}$ as in (14) in *V/f* source converters and using:

$$P_j = P_o - K_{fj}(f_j - f_{jo}) + \partial P_j^{ter} \quad (26)$$

$$\text{for } j = 1,2,\cdots,m$$

in *P/Q* source converters, with the integral action provided by:

$$\frac{d}{dt}(\partial P_i^{ter}) = -k_{ter}[g_i(P_i - P_{ref})] \quad (27)$$

$$\text{for } i = 1,2,\cdots,n+m-1$$

When tertiary control is activated, the active power sharing component $\eta_3$ introduced at the secondary frequency control needs to be deactivated, otherwise a conflict between secondary and tertiary control will arise.

## 6. Case Study AC Microgrid Model

The microgrid model implemented in MATLAB/Simulink will required to model the voltage source converters, to define a single line diagram for the islanded microgrid, and to define the topology network defined by its graph, for the frequency and voltage secondary control.

### A. *Voltage source converter and microgrid modelling*

Voltage source converters consist of both active switching devices such as insulated-gate bipolar transistors (IGBTs), with pulse width modulation (PWM) and passive components (LCL filters) to assist switching harmonic filtering. In distributed generation (DG) systems, VSCs are generally used with effective switching frequencies of a few thousand hertz for relatively low power applications.

For the V/f converters, a double-loop control will be used to ensure that the converter output voltage closely tracks the desired reference with both good transient and steady-state performance. An inner current loop functions by improving the overall system stability and attenuating the LC resonance introduced by the filter, and an outer voltage loop to improve reference voltage tracking. These two controllers will be classical PI controllers in the synchronous {d-q} frame, where fundamental components are dc signals, where $K_{p1}$ and $K_{i1}$ are the proportional and integral gain for the outer controller respectively, and $K_{p2}$ and $K_{i2}$ are the proportional and integral gain for the inner controller respectively.

For the P/Q converter, a state model for the VSC and the filter is designed in the synchronous {d-q} frame, where two PI controllers are implemented to control the output current in the LCL filter for each {d-q} component, providing a state vector, and an open-loop control input vector, defined by $\bar{x}$ , $\bar{u}$ respectively. A state feedback is applied to move the closed loop poles to a location four times faster than the open loop poles, given a feedback state gain $K$.

$$\bar{x} = [i_{i,d} \quad i_{i,q} \quad i_{o,d} \quad i_{o,q} \quad v_{cd} \quad v_{cq} \quad \varphi_d \quad \varphi_q]^t \quad (28)$$

$$\bar{u} = [v_{i,d} \quad v_{i,q}]^t \quad (29)$$

$$K^t = \begin{bmatrix} 43.9 & -22.3 \\ 31.4 & 41.6 \\ -38.9 & -18.5 \\ 59.8 & -9.5 \\ 3.8 & -7.9 \\ 12.9 & 4.9 \\ 8897 & -4400 \\ 4284 & 6635 \end{bmatrix} \quad (30)$$

The proposed control algorithms have been simulated in MATLAB/Simulink in the islanded AC microgrid described in

[16] (see Fig. 1). The microgrid consist of three DGs: two V/f source converters, and one P/Q source converter. Buses are connected by series RL branches. Line and load parameters are summarized in Table I.

*B. Graph topology*

For the secondary frequency control, only the V/f source converters will communicate with each other as in Fig. 2-a, where DG#2 is the leader agent (reference frequency of 50Hz).

The diagraph for the secondary voltage control for tracking a voltage profile, will communicate all the DGs with each other through as in Fig. 2-b. The three DGs will be leader agents, to track a voltage profile at the converter´s connection points.

The diagraph for the secondary voltage control for tracking the voltage at the PCC, will required an extra agent at the PCC communicated with all the DGs as in Fig. 2-c. The agent at the PCC will be the leader, to track a reference voltage.

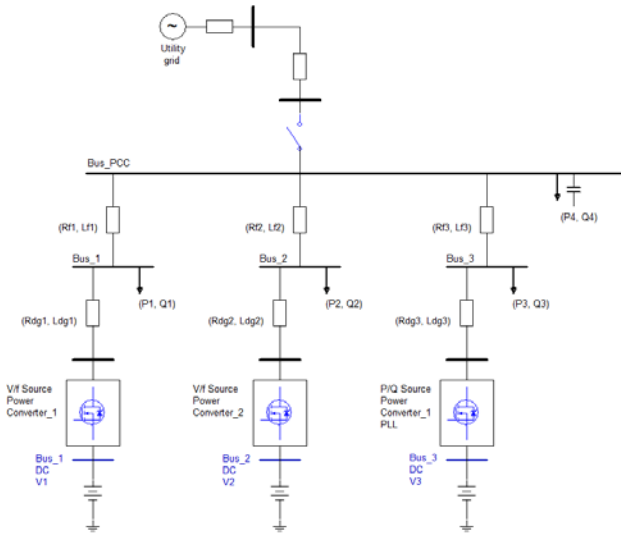


Fig. 1. Experimental AC microgrid.

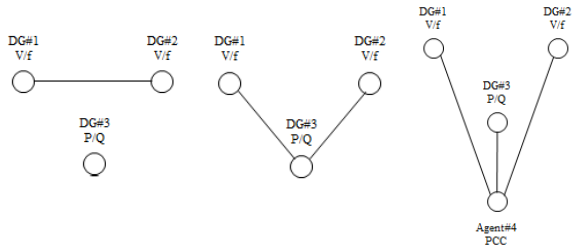


Fig. 2. Secondary control diagraphs.

Since there is no VSC at the PCC (agent#4), this agent can only communicate to the other DGs the voltage at the PCC.

## 7. Simulation Results

Simulation experiments have been carried out in the AC microgrid depicted in Fig. 1, for two cases.

*A. Case 1:* The simulation sequence is defined as follows: a load change in the PCC takes place at t=2s with only primary control activated. At t=4s and t=20s, secondary frequency and voltage controllers are activated, respectively, with a voltage profile set to the values of v_ref=[0.8;0.85;0.9] pu. Load change in the PCC at t=80s is doubled, and finally, a new load change in PCC is executed at t=160s (is reduced to half). See Fig. 3-6.

Table I. – Specifications of the microgrid model.

| | | | | | | |
|---|---|---|---|---|---|---|
| DGs | DG#1 V/f converter | | DG#2 V/f converter | | DG#3 P/Q converter | |
| | Rdg1 | 0.4 Ω | Rdg2 | 0.6 Ω | Rdg3 | 0.3 Ω |
| | Ldg1 | 6.6 mH | Ldg2 | 9.9 mH | Ldg3 | 5 mH |
| LCL filter | L1 | 1.5 mH | L1 | 1.5 mH | L1 | 1.5 mH |
| | L2 | 1.5 mH | L2 | 1.5 mH | L2 | 1.5 mH |
| | C | 20 µF | C | 20 µF | C | 20 µF |
| Outter loop | Kp1 | 5,00E-02 | Kp1 | 5,00E-02 | Eqs. (28-30) | |
| | Ki1 | 3,74E+02 | Ki1 | 3,74E+02 | | |
| Inner loop | Kp2 | 8,66E+00 | Kp2 | 8,66E+00 | | |
| | Ki2 | 0,00E+00 | Ki2 | 0,00E+00 | | |
| Lines | Line#1 | | Line#2 | | Line#3 | |
| | Rf1 | 0.757 Ω | Rf2 | 1.155 Ω | Rf3 | 0.678 Ω |
| | Lf1 | 3.1 mH | Lf2 | 6.2 mH | Lf3 | 1.6 mH |
| Loads | Load#1 | | Load#2 | | Load#3 | |
| | P1 | 1.21 MW | P2 | 0.6 MW | P3 | 1.5 MW |
| | Q1 | 0.81 kVA | Q2 | 0.42 kVA | Q3 | 0.95 kVA |
| | Load#4 (PCC) | | Sbase=10MVA Vbase=13.8kV | | | |
| | P4 | 0.9 MW | | | | |
| | Q4L | 0.61 kVA | | | | |
| | Q4C | -1.5 kVA | | | | |
| Primary Control | Kp1 | 4,00E+00 | Kp2 | 2,88E+00 | Kf3 | 3,00E-01 |
| | Kq1 | 3,00E-01 | Kq2 | 2,16E-01 | Kv3 | 4,00E+00 |

*B. Case 2:* The simulation sequence is as follows: a load change in PCC takes place at t=2s with only primary control activated. At t=4s and t=20s, secondary frequency and voltage controller to track the PCC at 1pu, are activated respectively. The synchronization controller at the PCC is switched on at t=80s (set point for the PCC angle is made equal to 1º). Finally, a new load change in PCC is executed at t=160s. See Fig. 7-11.

## 8. Conclusion

Secondary control based on multi-agents provides acceptable results for frequency and voltage restoration when communication delays are being neglected. It also makes it possible to synchronize the voltage phasor at the PCC prior to the connection to the utility grid. A trade-off between tracking a voltage profile, and reactive power sharing, needs to be reached. Similar trade-off should be taken for the tertiary control, and the active power sharing defined at the primary control. Future work should analyse the interactions between hierarchical control levels in an islanded hybrid AC/DC microgrid.

## Acknowledgement

S. Yagüe and A. García-Cerrada collaborate with the support of the project PRICAMCM (ref. S2013/IEC2933) partially financed by Madrid's Government."

## References

[1] Y. W. Li, “Control and resonance damping of voltage-source and current-source converters with LC filters," IEEE Trans. on Industrial Electronics, vol. 56, no. 5, pp. 1511-1521, 2009.

[2] J. Rocabert, A. Luna, F. Blaabjerg, and I. Paper, “Control of Power Converters in AC Microgrids," IEEE Transactions on Power Electronics, vol. 27, no. 11, pp. 4734-4749, 2012.

[3] A. Bidram, F. L. Lewis, A. Davoudi, and Z. Qu, “Frequency control of electric power microgrids using distributed ooperative control of multi-agent systems," 2013 IEEE Int. Conf. on Cyber Technology in Automation, Control and Intelligent Systems, pp. 223-228, 2013.

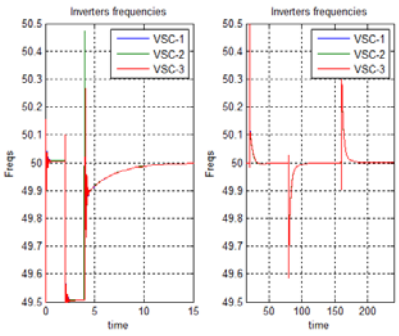


Fig. 3. Frequency (Case 1)

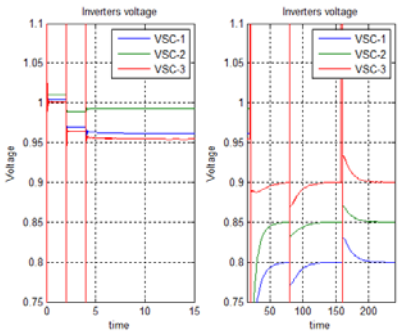


Fig. 4. Voltage profile (Case 1)

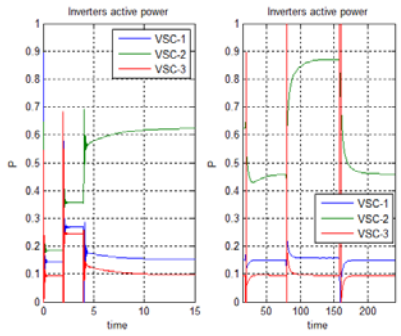


Fig. 5. Active power (Case 1)

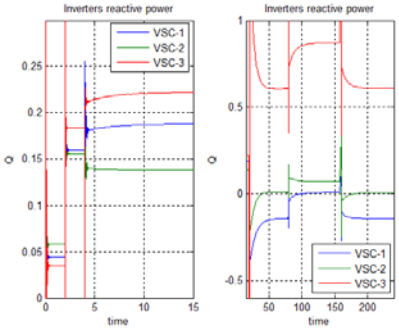


Fig. 6. Reactive power (Case 1)

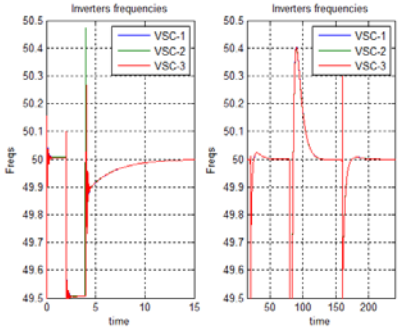


Fig. 7. Frequency (Case 2)

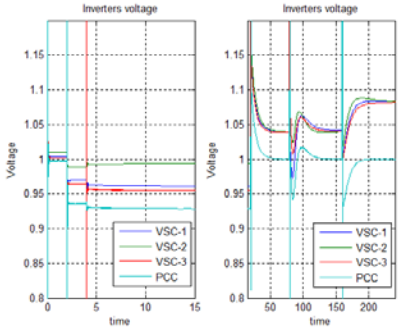


Fig. 8. Voltage profile (Case 2)

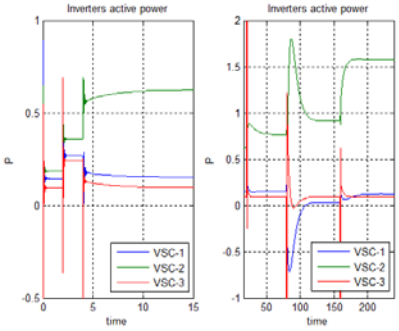


Fig. 9. Active power (Case 2)

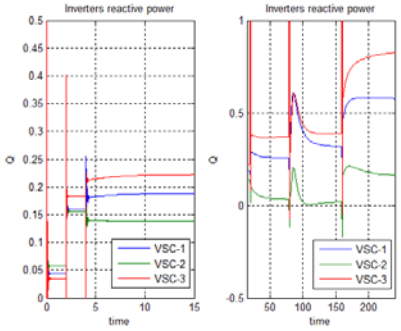


Fig. 10. Reactive power (Case 2)

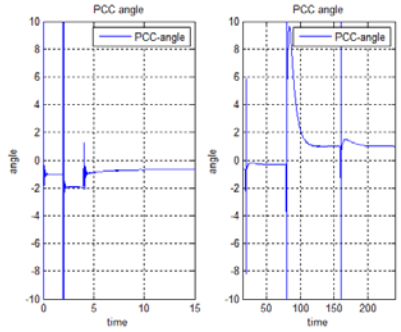


Fig. 11. PCC phase angle (Case 2)


[4] A. Bidram, A. Davoudi, F. L. Lewis, and J. M. Guerrero, “Distributed cooperative secondary control of microgrids using feedback linearization," IEEE Trans. on Power Systems, vol. 28, no. 3, pp. 3462-3470, 2013.

[5] F. Katiraei, M. R. Iravani, and P. W. Lehn, “Microgrid autonomous operation during and subsequent to islanding process," IEEE Trans. on Power Delivery, vol. 20, no. 1, pp. 248-257, 2005.

[6] A. Bidram and A. Davoudi, “Hierarchical structure of microgrids control system," IEEE Trans. on Smart Grid, vol. 3, no. 4, pp. 1963-1976, 2012.

[7] M. C. Chandorkar, D. M. Divan, and R. Adapa, “Control of parallel connected inverters in standalone ac supply systems," IEEE Trans. on Industry Applications, vol. 29, no. 1, pp. 136-143, 1993.

[8] N. Hatziargyriou, Microgrids: Architecture and Control, Wiley, 2014.

[9] M. Josep, J. C. Vasquez, Q. Sha_ee, S. Member, J. M. Guerrero, S. Member, and J. C. Vasquez, “Distributed Secondary Control for Islanded MicroGrids - A Novel Approach," IEEE Trans. on Power Electronic, 2014.

[10] K. H.-M. Frank L. Lewis, Hongwei Zhang and A. Das, Cooperative Control of Multi-Agent Systems. Springer, 2014.

[11] C. W. Reynolds, “Flocks, herds and schools: A distributed behavioral model,” ACM SIGGRAPH Computer Graphics, no. 4, pp. 25-34, 1987.

[12] K. H.-M. Frank L. Lewis, Hongwei Zhang and A. Das, Cooperative Control of Multi-Agent Systems. Springer, 2014.

[13] F. R. K. Chung, Spectral Graph Theory. American Mathematical Society, 1997.

[14] L. Gao, D. Cheng, and J. Wang, “On consensus of multiagent systems under dynamically changing interaction topologies,” 2007 IEEE Int. Conf. on Control and Automation, ICCA, pp. 7-11, 2008.

[15] J. W. Simpson-Porco, Q. Sha_ee, F. Dorer, J. C. Vasquez, J. M. Guerrero, and F. Bullo, “Secondary Frequency and Voltage Control of Islanded Microgrids via Distributed Averaging," IEEE Trans. on Industrial Electronics, vol. 62, no. 11, pp. 7025-7038, 2015.

[16] M. R. I. Katiraei, “Power management strategies for a microgrid with multiple distributed generation units," IEEE Trans. on Power Systems, vol. 21, no. 4, pp. 1821-1831, 2006.